Flexible Asymmetric Supercapacitors via Spray Coating of a New Electrochromic Donor–Acceptor Polymer

*Yitong Guo, Weishuo Li, Hongtao Yu, Dmitrii F. Perepichka, and Hong Meng**

Supercapacitors bridge the gap between batteries and traditional capacitors and have attracted attention as promising energy storage devices for their high rate capability.[1] At present, the energy density of supercapacitors is relatively low compared with batteries, which limits their practical applications.[2] Comparing to traditional electrode materials for supercapacitors, such as transition metal oxides, intrinsically conducting polymers have advantages of good conductivity, low cost, and flexibility.[3] Conducting polymers are "pseudo-capacitive," that is the energy storage involves a rapid redox reaction in the bulk of the material. This provides a superior specific energy to carbonaceous materials[4] that store energy through a physical process of charge accumulation in the electric double layer at the electrode–electrolyte surface. Different types of conducting polymers could be used in supercapacitors, including polyaniline (PANI), polypyrrole (PPy), polythiophene, and their derivatives.[3,5] The wide tunability of polymer structure offers an opportunity to develop new electrode materials with enhanced capacitance and good stability, pointing out a promising way of achieving supercapacitors with higher energy. The intrinsic flexibility of conducting polymers has made them favored materials in flexible and lightweight energy storage devices, which play an important role in future portable and wearable electronic devices.[6]

Electrochemical redox properties of π-conjugated polymers can be controlled by tailoring their molecular structures.[7] Donor–acceptor (D–A) conjugated polymers are a unique type of materials in which electron donor and acceptor building blocks can be selected at will,[8] which allows to tune the band gap and has been proved as an effective strategy in organic photovoltaics (OPVs),[9] polymer light-emitting diodes,[10] electrochromics,[11] and chemical sensors.[12] However, applications of D–A polymers for energy storage applications are still very rare.[13]

Herein we report a new donor–acceptor electroactive polymer, poly[4,7-bis(3,6-dihexyloxy-thieno[3,2-*b*]thiophen-2-yl)]-benzo[*c*][1,2,5]thiadiazole (PBOTT-BTD) applied as an electrode material to build supercapacitor devices of considerable capacitance and stability. Different from previously reported pseudocapacitive D–A polymers adopting (3,4-ethylenedioxythiophene) (EDOT) as the donor building block,[13] we introduce 3,6-dihexyloxythieno[3,2-*b*]thiophene instead as the donor unit in PBOTT-BTD. Poly(3,6-dialkoxythieno[3,2-*b*]thiophene) homopolymer has been reported previously as a possible alternative to poly(3,4-ethylenedioxythiophene) (PEDOT),[14] but has not been studied in energy-storage devices. This is the first time we introduce 3,6-dialkoxythieno[3,2-*b*]thiophene as the donor building block in pseudocapacitive D–A polymers. The electroactive polymer PBOTT-BTD exhibits favorable redox activity, good stability and solubility, expanding the "tool-box" of donor building blocks for D–A conjugated polymers. Distinct from other state-of-the-art electrode materials prepared through an electrochemical polymerization method,[15] PBOTT-BTD is solution processable and can be easily spray coated on flexible indium tin oxide (ITO) coated polyethylene terephthalate (PET) substrates, providing a possibility for high-throughput processing on a large scale. Interestingly, PBOTT-BTD displays a dual energy storage/electrochromic functionality: the charging/discharging of the polymer electrode can be visually monitored by color change, realizing a "smart" energy storage device. We applied PBOTT-BTD as the positive electrode material and PEDOT as the negative electrode material in fabricating conducting polymer-based flexible asymmetric supercapacitors.

The synthetic route from thieno[3,2-*b*]thiophene to PBOTT-BTD is shown in **Scheme 1**. Tetrabromothieno[3,2-*b*]thiophene (**1**), 3,6-dibromothieno[3,2-*b*]thiophene (**2**), and 3,6-dimethoxythieno[3,2-*b*]thiophene (**3**) were prepared in satisfactory yields according to previously reported work.[16] 3,6-Dihexyloxythieno[3,2-*b*]thiophene (**4**) was obtained via a transetherification reaction from **3**. Stannylation of **4** afforded **5** which was used without further purification in the next step. The D–A–D monomer (**M1**) was prepared via a Stille coupling reaction between **5** and 4,7-dibromobenzo[*c*][1,2,5]thiadiazole in toluene with $Pd(PPh_3)_4$ as catalyst, and its dibromo derivative (**M2**) was obtained by bromination with n-bromosuccinimide (NBS). The molecular structures of **M1** and **M2** were confirmed by ^1H and ^{13}C NMR spectra and mass spectra (MS) measurements (see the Supporting Information). The "green" C—H arylation polycondensation of **M1** and **M2** was carried out in dimethylacetamide with $Pd(OAc)_2$ as catalyst and K_2CO_3 as base without any ligand. PBOTT-BTD was obtained in 56% yield after purification by Soxhlet extraction. The structure of the polymer was confirmed by ^1H NMR spectra (the Supporting Information) and the molecular weight determined by gel permeation chromatography were M_w = 3626 Da, M_n = 3431 Da, and polydispersity index (PDI) = 1.1.

PBOTT-BTD was dissolved in chloroform at 0.5 mg mL^{-1} concentration and the solution was carefully spray coated

Y. Guo, W. Li, Dr. H. Yu, Prof. H. Meng
School of Advanced Materials
Peking University Shenzhen Graduate School
Shenzhen 518055, China
E-mail: menghong@pkusz.edu.cn
Prof. D. F. Perepichka
Department of Chemistry and Center for
Self-Assembled Chemical Structures
McGill University
Montreal H3A 0B8, QC, Canada

DOI: 10.1002/aenm.201601623

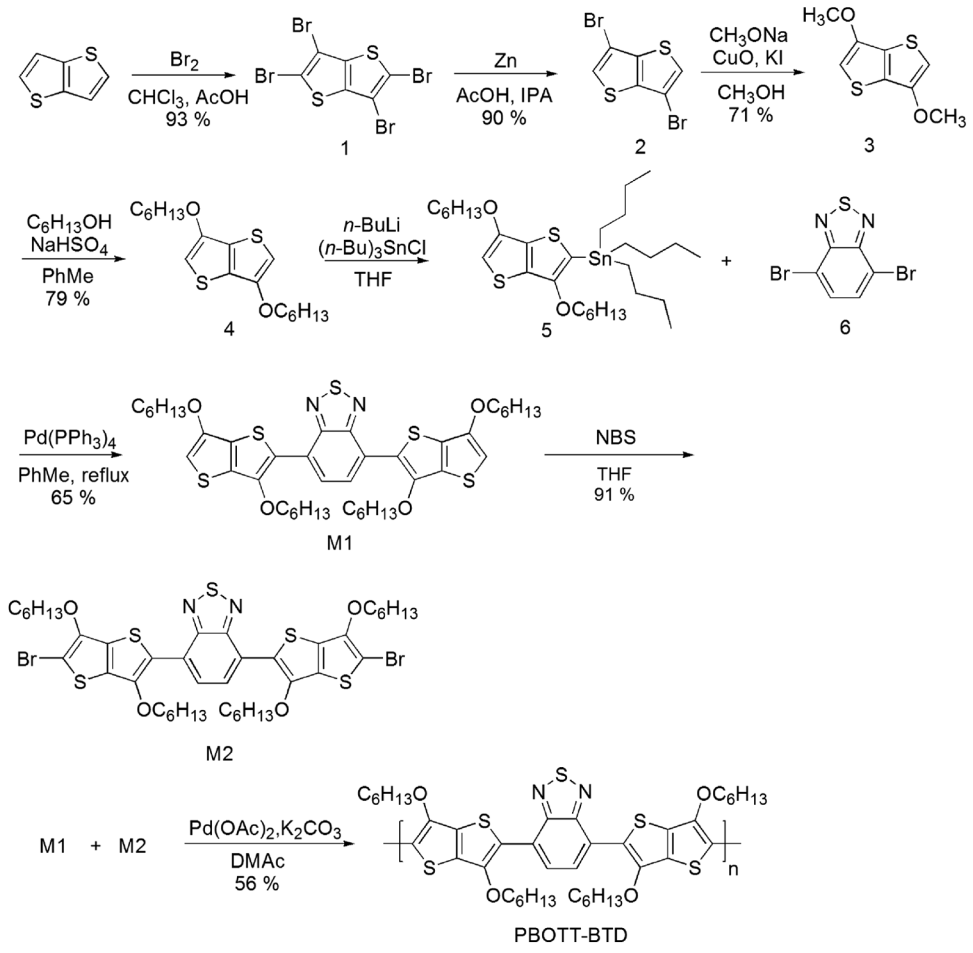

Scheme 1. Synthetic route to PBOTT-BTD.

on a flexible ITO/PET substrate to form a uniform film. The spray coated PBOTT-BTD/ITO/PET was used as working electrode and measured in a three-electrode configuration in 0.1 M $TBAPF_6$/acetonitrile (ACN) solution. The cyclic voltammetry (CV) experiments were carried out between –0.4 and 0.6 V (vs Ag/Ag^+) at different scan rates from 10 to 200 mV s^{-1} (**Figure 1**a). The CV curves of the polymer have a near-ideal shape for energy storage applications: a broad flat current across a wide potential range (from –0.2 to 0.6 V) and sharp redox onsets. This is highly favorable for a stable power output throughout the discharging process. The polymer film exhibits an oxidation onset at –0.10 V and two pairs of redox peaks (E_{pa1} = 0.03 V, E_{pc1} = –0.08 V; E_{pa2} = 0.40 V, E_{pc2} = 0.32 V) at 50 mV s^{-1} scan rate. The symmetry between the cathodic/anodic peaks indicates good reversibility of the redox reactions in charging/discharging of the polymer electrode. This reversible redox behavior over a wide potential window (1.0 V) indicates that PBOTT-BTD is a potential suitable material for electrochemical supercapacitors.[3] At an active material mass loading of 0.08 mg cm^{-2}, the PBOTT-BTD/ITO/PET electrode exhibits a maximum area capacitance of 2.5 mF cm^{-2} measured by galvanostatic charge–discharge (CD) at a current density of 0.1 mA cm^{-2} (Figure 1b,c). The corresponding specific capacitance of PBOTT-BTD is evaluated to be 31 F g^{-1}. This is comparable with the peak capacitance values reported for other donor–acceptor polymers electrodes.[13] The specific capacitance is measured for a relative thick film (in which some polymer chains may not fully participate in the charge–discharge process) and can be potentially further improved by engineering the film structures and making composites. As a supercapacitor electrode material, PBOTT-BTD has good cyclic stability: 86% of capacitance is maintained after 2000 cycles between –0.4 and 0.6 V (scan rate of 200 mV s^{-1}) in ambient air (**Figure 2**d).

The thickness of the spray coated film has been optimized to achieve maximum capacitance as supercapacitor electrode. The film thickness can be controlled by adjusting the spray coating time and we investigated the effect of film thickness on single electrode capacitance. As the film thickness increases, area capacitance of the PBOTT-BTD/ITO/PET electrode first increases due to higher loading of the material and then approaches a saturated value due to limited conductivity/ion permeability of the polymer (Figure S1, Supporting Information). The optimal film thickness of PBOTT-BTD on ITO/PET was found to be about 300 nm. The scanning electron microscope (SEM) imaging of the spray coated polymer shows a twisted fiber structure (Figure 2b). This porous structure is favorable for providing a larger contact area between the electrode material and electrolyte as well as buffering the

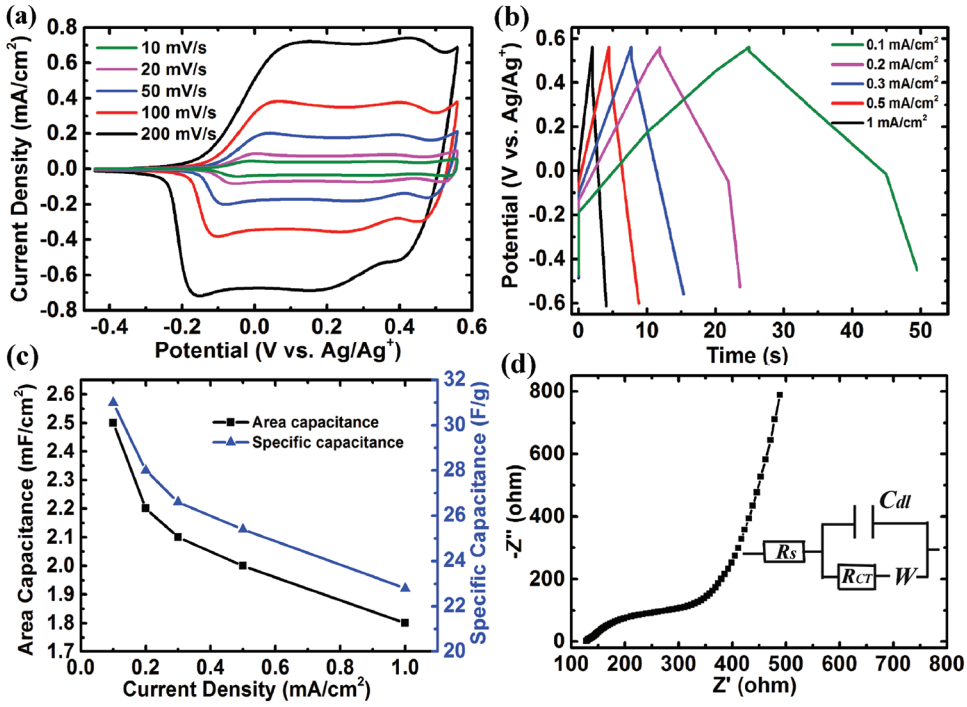

Figure 1. Electrochemical behaviors of the PBOTT-BTD/ITO/PET electrode in a three-electrode configuration. a) CV and b) galvanostatic CD curves. c) Area capacitance and specific capacitance of PBOTT-BTD calculated from galvanostatic charge–discharge at different current densities. d) Nyquist plots of the PBOTT-BTD/ITO/PET electrode. Inset is the Randles equivalent circuit.

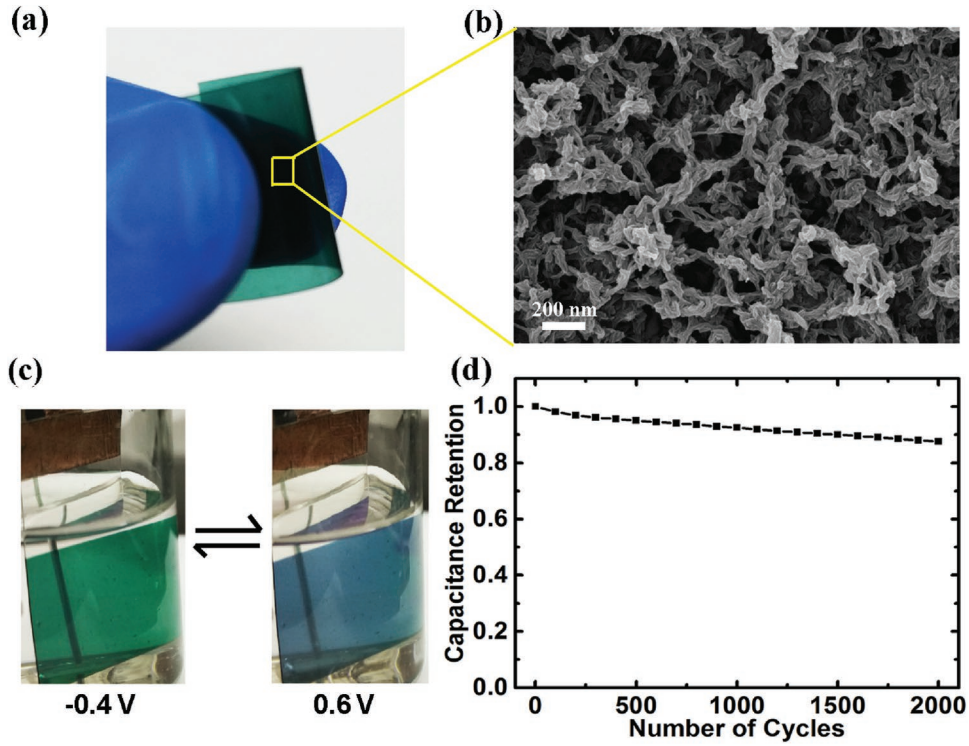

Figure 2. a) Photograph of the PBOTT-BTD/ITO/PET flexible electrode. b) SEM image of the spray coated polymer. c) Color change between discharged (–0.4 V, green) and charged (0.6 V, blue) state. d) Stability of PBOTT-BTD spray coated on Pt disk electrode measured in 0.1 M $TBAPF_6$/ACN solution in ambient air through CV at a scan rate of 200 mV s^{-1}.

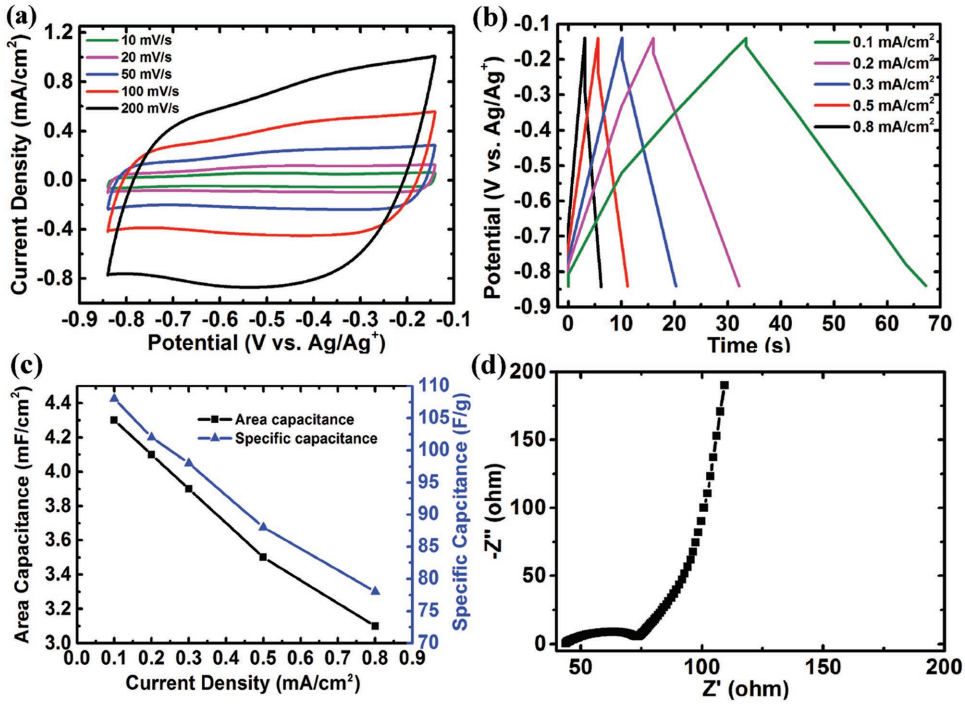

Figure 3. Electrochemical behaviors of the PEDOT/ITO/PET electrode in a three-electrode configuration. a) CV and b) galvanostatic charge–discharge curves. c) Area capacitance and specific capacitance of electropolymerized PEDOT (1 min) calculated from the galvanostatic charge–discharge curves at different current densities. d) Nyquist plots of the PEDOT/ITO/PET electrode.

volume change of electrode material during charging and discharging, which is essential for cyclic stability of the polymer electrode.[3,17] Interestingly, besides the energy storage capacity, our polymer also shows distinct electrochromic properties. As shown in Figure 2c, the polymer film appears green in its uncharged state (–0.4 V) and changes to blue after charging (0.6 V). The color change during charging is associated with formation of polarons and bipolarons that possess a longer-wavelength absorption.[7] This obvious and reversible color signal visually exhibits the charged or discharged state of the electrode, realizing a "smart" energy storage device, which has become a recent research hotspot.[18]

PEDOT has been widely studied as an electrode material in supercapacitors for its considerable capacitance, wide potential window, high conductivity, and stability. The specific capacitance of PEDOT is lower than that of PANI and PPy due to its relatively large molecular weight and low doping level.[3] However, PEDOT is electroactive over a particularly wide potential window (nearly 2.0 V), which enables it to serve as both positive and negative electrode material in principle. PEDOT has been explored as the positive electrode in most of previous work.[5c,19] In our experiments, we observed that PEDOT is stable until a negative potential of –0.8 V (vs Ag/Ag^+) at which is existed in the neutral state (n-doping of PEDOT occurs below –1.5 V and the n-doped state is not stable even in water/oxygen-free environment).[20] Considerable capacitance and high stability in the negative potential range makes PEDOT a suitable negative electrode material to complement p-doped PBOTT-BTD in an asymmetric supercapacitor.

PEDOT film on a flexible ITO/PET substrate was prepared by electrochemical polymerization at a constant potential of 1.0 V. The electrodeposition time was selected as 1 min in the consideration of charge balance between the negative and positive electrodes. We characterized the PEDOT electrode in a negative potential range of –0.8 to –0.1 V in a three-electrode configuration (**Figure 3**). With a mass loading of 0.04 mg cm^{-2}, the PEDOT electrode shows an area capacitance of 4.3 mF cm^{-2} and specific capacitance of 108 F g^{-1} at a current density of 0.1 mA cm^{-2}.

Two PBOTT-BTD/ITO/PET electrodes of the same optimized film thickness are assembled in a symmetric supercapacitor device. The symmetric supercapacitor provides a 0.6 V operating voltage and an energy density of 0.3 W h kg^{-1} at 0.2 mA cm^{-2}. In conducting polymer-based pseudocapacitors, this type of symmetric device is also referred to as type I device, in which the same p-dopable polymer is used for both electrodes.[3] In the charged state of type I device, the positive electrode is in its fully oxidized form while the negative electrode is in the neutral state. When fully discharged, both electrodes are in half-oxidized states, and so only 50% of electrode material's total capacitance can be used.[17] This type of device has a relatively low voltage and the energy it can provide is limited. To further exploit the capacitance of PBOTT-BTD and raise the operating voltage, we have fabricated PBOTT-BTD//PEDOT asymmetric supercapacitors, which belong to type II devices (asymmetric devices using two different p-dopable polymers with a different range of electroactivity). This type II device owns both advantages of elevating operating voltage as compared with type I device and avoiding employment of unstable n-doped polymers as compared with type III devices (symmetric devices applying the same polymer for both electrodes with the p-doped form as positive electrode and n-doped form as negative electrode).[3]

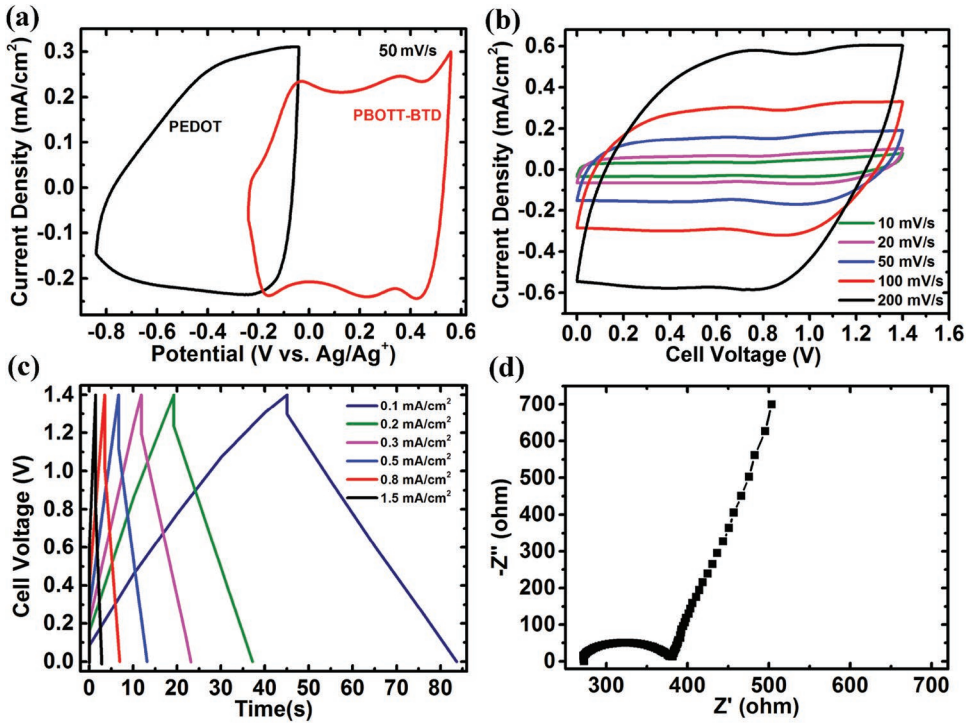

Figure 4. a) CV curves of the PBOTT-BTD/ITO/PET and PEDOT/ITO/PET electrode in 0.1 M $TBAPF_6$/ACN. b) CV and c) galvanostatic charge–discharge curves of the asymmetric supercapacitor. d) Nyquist plots of the asymmetric supercapacitor.

It was found that PBOTT-BTD as the positive electrode and PEDOT as the negative electrode cooperate well in an all-polymer asymmetric supercapacitor. The representative CV curves of PBOTT-BTD and PEDOT in the positive and negative potential region are shown in **Figure 4**a. The amount of charge for both electrodes is matched by adjusting the thickness of the PEDOT electrode. The CV curves of the asymmetric supercapacitor have a near-ideal rectangular shape, as shown in Figure 4b, revealing good capacitive properties and charge–discharge symmetry of the asymmetric device. The asymmetric device provides a 1.4 V operating voltage, more than twice as high as that of PBOTT-BTD-based symmetric device. The asymmetric supercapacitor achieves a maximum energy density of 6.3 W h kg^{-1} at 0.8 A g^{-1}. And an energy of 3.5 W h kg^{-1} is maintained at a high power of 8.8 kW kg^{-1} (at 12.5 A g^{-1}), showing good rate capability of the devices. The energy density of our asymmetric device is comparable to the electropolymerized donor–acceptor polymer-based type III devices reported by Reynolds group (9–15 W h kg^{-1})[13a] and Seferos group (3.6–11 W h kg^{-1})[13b] with additional advantages of solution processability and higher stability. Those type III devices employing unstable n-doped polymers have poor cyclic stability, showing severe decay after 100 cycles,[13] which greatly hampers their practical applications. Compared with the solution processed PEDOT analogues-based supercapacitors (4–18 W h kg^{-1}, 0.8–3.3 kW kg^{-1}) recently reported by Reynolds group,[21] our asymmetric device achieves a similar energy density but a higher power density.

Comparison between the PBOTT-BTD-based symmetric supercapacitor and PBOTT-BTD//PEDOT asymmetric supercapacitor, including their operating voltage, specific capacitance, specific energy, and power are listed in **Table 1**. The asymmetric devices provide significantly improved operating voltage, specific energy, and power compared with the symmetric ones, indicating that PBOTT-BTD and PEDOT, having complementary potential windows, cooperate well in the all-polymer asymmetric supercapacitor. Meanwhile, it can be noticed that capacitance of the supercapacitor device is lower than that of the single electrode measured in a three-electrode configuration. This capacitance loss can be explained by the nonideal conditions in the devices, including the overall series resistance arising from imperfect electric contacts.[13a] It can be observed from the Nyquist plots (Figure 4d) that the internal resistance in the device has increased compared with that of single electrode, with the intercept with Z' axis presenting 272 Ω.

A relatively low energy compared with batteries is a key challenge for expanding the practical applications of supercapacitors.[1] According to $E = CV^2/2$ (E is energy density, C is capacitance, and V is potential window), boosting the operating voltage will bring about a twofold increase in energy density. For conducting polymer-based supercapacitors, type III/IV devices, which applied the same/different p- and n-doped polymer for positive and negative electrode, can achieve a high cell voltage

Table 1. Performance of PBOTT-BTD-based symmetric and PBOTT-BTD//PEDOT asymmetric supercapacitors. Measured from galvanostatic discharge at 0.2 mA cm^{-2}.

	Voltage [V]	C [F g^{-1}]	W_S [W h kg^{-1}]	P_S [kW kg^{-1}]
Sym metric device	0.6	8	0.3	0.2
Asymmetric device	1.4	21	5.7	1.2

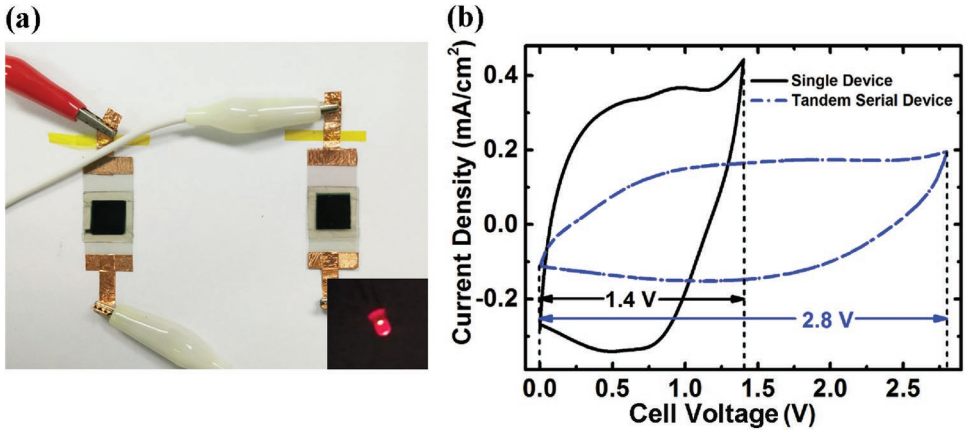

Figure 5. a) Two asymmetric PBOTT-BTD//PEDOT supercapacitors connected in series. Inset shows a red LED bulb lighted by two serial devices. b) CV curves of the single asymmetric supercapacitor and two serial devices in tandem, at 100 mV s^{-1}.

of 2.0–3.0 V.[3] However, the employment of unstable n-doped polymers compromises the stability of these devices, which is still far below the demands of practical applications. In our all-polymer asymmetric supercapacitors employing one of the most stable conducting polymers, PEDOT, as the negative electrode, a moderate 1.4 V voltage has been achieved. We further increase the voltage by connecting two supercapacitors head-to-tail in series and a 2.8 V voltage is achieved, an expected two-fold increase compared with the single device (**Figure 5**b). Two asymmetric supercapacitors connected in series are applied as the power source to light a red light-emitting diode (LED) (3 mm diameter, 1.8 V turn-on voltage) (Figure 5a). After charging at 2.8 V for 10 s, the tandem supercapacitors can light the LED for about 15 s.

In summary, we have synthesized a thieno[3,2-*b*]thiophene-based donor–acceptor polymer PBOTT-BTD. This electroactive polymer has a moderate capacitance and good stability across a wide potential window of 1.0 V and is applied as a positive electrode material in all-polymer asymmetric supercapacitors. This is the first time we introduce 3,6-dialkoxy-thieno[3,2-*b*]thiophene as the donor building block in energy-storage polymers. The alkoxy chains increase solubility of the polymer, enabling easy processing of PBOTT-BTD via spray coating on flexible ITO/PET substrates. A distinct electrochromic behavior of this polymer leads to a "smart" energy storage device in which the charged/discharged state can be visually monitored. We select PEDOT, a popular conducting polymer with a wide potential window and high stability as the negative electrode to complement PBOTT-BTD in fabricating all-polymer asymmetric flexible supercapacitors. The PBOTT-BTD//PEDOT supercapacitors provide an energy density of 3.5–6.3 W h kg^{-1} and a power density of 0.6–8.8 kW kg^{-1}, exhibiting significant increase compared with the PBOTT-BTD-based symmetric device. This strategy of applying PEDOT in the negative potential range as negative electrode provides useful reference for designing new types of asymmetric supercapacitors.

Experimental Section

Materials: All chemicals for synthesizing PBOTT-BTD were purchased from Aldrich. Dichloromethane and ACN were predried over activated 4A molecular sieves and refluxed over calcium hydride for 2 h before distillation. ITO/PET plastic sheets (thickness of 125 µm and square resistance of 18 Ω □$^{-1}$) were employed as flexible conductive substrates for making supercapacitor devices. Tetra-*n*-butylammonium hexafluorophosphate ($TBAPF_6$) was purchased from J&K Chemical Co. Polymethylmethacrylate (PMMA) was purchased from Aladdin. Anhydrous propylene carbonate (PC) of 99.7% purity was used as received from Sigma-Aldrich.

Electrode Preparation and Characterization: PBOTT-BTD was fully dissolved in chloroform to get 0.5 mg mL^{-1} solution and the solution was filtered *via* filter membrane of 0.22 µm pore diameter, to remove any undissolved substance and avoid spray nozzle blockage. A steady airflow was kept during spray coating to get a uniform film on ITO/PET substrates. The film thickness was measured by a profilometer (BRUKER DEKTAK XT, Germany). PEDOT was prepared through electrochemical polymerization in a three-electrode cell with ITO/PET as the working electrode, Pt wire as the counter electrode and Ag wire as the quasi-reference electrode. The electrolyte was 0.1 M $TBAPF_6$/ACN solution containing 0.02 M EDOT. Potential of the Ag wire was calibrated versus the Fc/Fc^+ redox couple standard (+0.52 V vs Ag wire, +0.08 V vs Ag/Ag^+ nonaqueous reference electrode). And all the potentials in the Results and Discussion part were presented as potentials vs Ag/Ag^+ nonaqueous electrode (containing 10 mM $AgNO_3$/ACN solution). EDOT was electrochemically polymerized potentiostatically at 1.0 V (vs Ag/Ag^+) for 1 min. Both electropolymerization and CV experiments were performed using a CHI620E Electrochemical Workstation, Shanghai Chenhua Corporation. The mass of active material PBOTT-BTD on ITO/PET was weighed in triplicate using a Mettler Toledo semimicroanalytical balance ($\triangle m = \pm 0.01$ mg). The mass of PEDOT is too little to be weighed accurately and thus the mass was calculated approximately following the equation below, assuming a 100% current efficiency (η)[22]

$$m = \frac{(\eta Q_{dep})M}{FZ} \quad (1)$$

where M is the molecular weight of EDOT. F is the Faraday constant (96,485 C mol^{-1}). Z is the number of electrons transferred per monomer attached to the polymer and $Z = 2 + f$. The partial charge f is called doping level, which has been reported as 0.33 for PEDOT.[3]

All electrochemical characterization of single electrodes (CV, galvanostatic charge–discharge and electrochemical impedance spectrometry) was carried out in a three-electrode cell containing 0.1 M $TBAPF_6$/ACN electrolyte solution. The galvanostatic CD was carried out using a Maccor Model MC-16 Battery Test System. The electrochemical impedance spectrometry (EIS) was carried out using Solartron Electrochemical Workstation. EIS was performed in the frequency range from 100 kHz to 0.1 Hz at the open circuit potential by applying a small sinusoidal potential of 5 mV signal. The surface morphology of the

active material on ITO/PET was imaged by a SEM (ZEISS SUPRA 55, Germany).

Supercapacitor Devices Fabrication: In making a supercapacitor device, the edges of two polymer/ITO/PET sheets were first sealed with a 3M double-side tape, leaving a small gap for injecting the gel electrolyte. Overlap area of both electrodes in each device is 1 cm^2. 0.2 M $TBAPF_6$ in 7% m/v PMMA in PC was used as gel electrolyte. No separator paper was needed in our devices. The symmetric supercapacitor was assembled with two spray coated PBOTT-BTD/ITO/PET electrodes. Before assembly the electrode that was to comprise the positive electrode was held at 0.6 V (vs Ag/Ag^+) for 30 s and the negative electrode was held at –0.4 V (vs Ag/Ag^+) for 30 s. The asymmetric device was assembled with PBOTT-BTD/ITO/PET as the positive electrode and PEDOT/ITO/PET as the negative electrode. Both electrodes were held at –0.2 V for 30 s before assembling the device. All device assembly processes were carried out in air.

The performance of symmetric and asymmetric supercapacitors were evaluated by CV, galvanostatic charge–discharge and EIS in a two-electrode configuration in air. Two asymmetric supercapacitors were connected in series for lighting a red LED bulb (3 mm diameter and 1.8 V turn-on voltage).

Supporting Information

Supporting Information is available from the Wiley Online Library or from the author.

Acknowledgements

This work was financially supported by Shenzhen Key Laboratory of Organic Optoelectromagnetic Functional Materials of Shenzhen Science and Technology Plan (ZDSYS20140509094114164), the Shenzhen Peacock Program (KQTD20140627145432 96), Shenzhen Science and Technology Research Grant (JCYJ20140509093817690), Shenzhen Science and Technology Research Grant (JCYJ20160331095335232), Nanshan Innovation Agency Grant (KC2015ZDYF0016A), Guangdong Key Research Project (No. 2014B090914003 and 2015B090914002), and National Basic Research Program of China (973 Program, No. 2015CB856505). The authors thank Haibo Su and Prof. Rong Sun at Shenzhen Institutes of Advanced Technology Chinese Academy of Science for advice in device fabrication.

Received: July 25, 2016
Revised: August 23, 2016
Published online: October 10, 2016

[1] P. Simon, Y. Gogotsi, *Nat. Mater.* **2008**, *7*, 845.
[2] a) D. P. Dubal, O. Ayyad, V. Ruiz, P. Gómez-Romero, *Chem. Soc. Rev.* **2015**, *44*, 1777; b) G. Wang, L. Zhang, J. Zhang, *Chem. Soc. Rev.* **2012**, *41*, 797.
[3] G. A. Snook, P. Kao, A. S. Best, *J. Power Sources* **2011**, *196*, 1.
[4] F. Béguin, V. Presser, A. Balducci, E. Frackowiak, *Adv. Mater.* **2014**, *26*, 2219.
[5] a) Z. Yu, L. Tetard, L. Zhai, J. Thomas, *Energy Environ. Sci.* **2015**, *8*, 702; b) N. Kurra, R. Wang, H. N. Alshareef, *J. Mater. Chem. A* **2015**, *3*, 7368; c) B. Anothumakkool, R. Soni, S. N. Bhange, S. Kurungot, *Energy Environ. Sci.* **2015**, *8*, 1339; d) H. Cong, X. Ren, P. Wang, S. Yu, *Energy Environ. Sci.* **2013**, *6*, 1185; e) X. Xia, D. Chao, Z. Fan, C. Guan, X. Cao, H. Zhang, H. Fan, *Nano Lett.* **2014**, *14*, 1651.
[6] a) L. Nyholm, G. Nyström, A. Mihranyan, M. Strømme, *Adv. Mater.* **2011**, *23*, 3751; b) X. Lu, M. Yu, G. Wang, Y. Tong, Y. Li, *Energy Environ. Sci.* **2014**, *7*, 2160; c) I. Shown, A. Ganguly, L. Chen, K. Chen, *Energy Sci. Eng.* **2015**, *3*, 2; d) B. C. Kim, J. Hong, G. G. Wallace, H. Park, *Adv. Energy Mater.* **2015**, *5*, 1500959.
[7] T. A. Skotheim, J. R. Reynolds, *Handbook of Conjugated Polymers*, 3rd ed., CRC, Boca Raton, FL **2007**.
[8] a) E. E. Havinga, W. Hoeve, H. Wynberg, *Polym. Bull.* **1992**, *29*, 119; b) P. M. Beaujuge, C. M. Amb, J. R. Reynolds, *Acc. Chem. Res.* **2010**, *43*, 1396.
[9] a) T. M. Clarke, J. R. Durrant, *Chem. Rev.* **2010**, *110*, 6736; b) B. C. Thompson, J. M. J. Fréchet, *Angew. Chem., Int. Ed.* **2008**, *47*, 58.
[10] A. C. Grimsdale, K. L. Chan, R. E. Martin, P. G. Jokisz, A. B. Holmes, *Chem. Rev.* **2009**, *109*, 897.
[11] P. M. Beaujuge, J. R. Reynolds, *Chem. Rev.* **2010**, *110*, 268.
[12] R. A. Potyrailo, *Angew. Chem., Int. Ed.* **2006**, *45*, 702.
[13] a) L. A. Estrada, D. Y. Liu, D. H. Salazar, A. L. Dyer, J. R. Reynolds, *Macromolecules* **2012**, *45*, 8211; b) P. M. DiCarmine, T. B. Schon, T. M. McCormick, P. P. Klein, D. S. Seferos, *J. Phys. Chem. C* **2014**, *118*, 8295.
[14] a) M. Turbiez, P. Frère, P. Leriche, N. Mercier, J. Roncali, *Chem. Commun.* **2005**, *9*, 1161; b) L. D. Cremer, T. Verbiest, G. Koeckelberghs, *Macromolecules* **2008**, *41*, 568.
[15] a) J. C. Bachman, R. Kavian, D. J. Graham, D. Y. Kim, S. Noda, D. G. Nocera, Y. Shao-Horn, S. W. Lee, *Nat. Commun.* **2015**, *6*, 1; b) H. Zhang, Y. Zhang, C. Gu, Y. Ma, *Adv. Energy Mater.* **2015**, *5*, 1402175.
[16] a) C. R. G. Grenier, WO 2012/058209 A1, **2012**; b) L. S. Fuller, B. Iddon, K. A. Smith, *J. Chem. Soc., Perkin Trans. 1* **1997**, *22*, 3465; c) N. Hergue, P. Frere, J. Roncali, *Org. Biomol. Chem.* **2011**, *9*, 588.
[17] F. Béguin, E. Frackowiak, Z. Zhang, *Supercapacitors: Materials, Systems, and Applications*, China Machine Press, Beijing **2014**.
[18] a) G. Cai, P. Darmawan, M. Cui, J. Wang, J. Chen, S. Magdassi, P. S. Lee, *Adv. Energy Mater.* **2015**, *5*, 1501882; b) X. Chen, H. Lin, J. Deng, Y. Zhang, X. Sun, P. Chen, X. Fang, Z. Zhang, G. Guan, H. Peng, *Adv. Mater.* **2014**, *26*, 8126; c) J. Zhao, Y. Tian, Z. Wang, S. Cong, D. Zhou, Q. Zhang, M. Yang, W. Zhang, F. Geng, Z. Zhao, *Angew. Chem., Int. Ed.* **2016**, *55*, 7161.
[19] Z. Zhao, G. F. Richardson, Q. Meng, S. Zhu, H. Kuan, J. Ma, *Nanotechnology* **2016**, *27*, 042001.
[20] H. J. Ahonen, J. Lukkari, J. Kankare, *Macromolecules* **2000**, *33*, 6787.
[21] A. M. Österholm, J. F. Ponder Jr., J. A. Kerszulis, J. R. Reynolds, *ACS Appl. Mater. Interfaces* **2016**, *8*, 13492.
[22] D. Mo, W. Zhou, X. Ma, J. Xu, *Electrochim. Acta* **2015**, *155*, 29.

